

Department of Electrical and Computer Engineering

University of Victoria

ELEC 360 - Control Systems I

LABORATORY REPORT

Experiment No.:	1
Title:	Modeling and Parameter Identification of a DC Motor
Date of experiment:	4 October, 2016
Report submitted on:	11 October, 2016
To:	Amirhosein Khazenifard, B04
Lab Group No.:	44
Names:	A.-K. Blanken (V00809798) T. Stephen (V00812021) S. Todesco (V00821678)

1 Summary

Three methods are presented for determining the gain K and time constant τ of the first order linear model of a DC motor. The angular velocity of the motor ω_m is related to the input voltage u_m through the model. An analytical derivation with approximate values for the physical elements of the motor yields poor results. Using analysis of static conditions on the experiment motor yields an acceptable model that underestimates its velocity at higher input voltage. The bump test, which measures the system's response to a unit step input, gives a highly accurate model with $K = 18.8 \text{ rad V}^{-1} \text{ s}^{-1}$ and $\tau = 0.091 \text{ s}$.

2 Introduction

This experiment will develop a model for a DC motor controller. The angular velocity of a DC motor in an armature configuration, shown in Figure 1, can be approximated by a first order system. We can vary the applied voltage u_m in a static configuration to determine the internal resistance of the particular motor R_m and its torque constant k_m . These two values let us determine the the gain K and time constant τ of the governing first order equation

$$G(s) = \frac{K}{\tau s + 1}. \quad (1)$$

This model will be improved by analyzing the system input and output under dynamic conditions. Measurements in dynamic conditions make fewer assumptions about the system and give a better approximation for K and τ .

The QICii software package measures the motor's response to different u_m inputs. It will also compare the actual response to an expected response determined by user-defined K and τ .

The parameters derived in this experiment will be used for modeling more complex control structures in subsequent experiments.

Table 1 summarizes the relevant physical parameters in Figure 1. Relevant equations describing the behavior of the motor will be introduced throughout Section 4 as they are required.

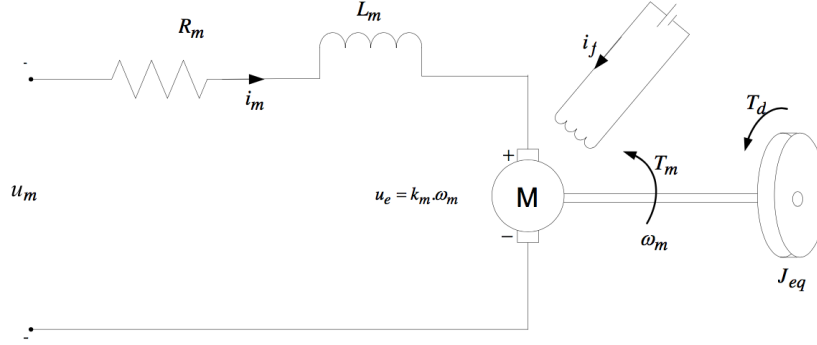


Figure 1: DC Motor in armature configuration

Table 1: DC Motor system nomenclature

Symbol	Description	Units
ω_m	Motor angular velocity	rad s^{-1}
u_m	Voltage from amplifier which drives motor	V
u_e	Back-emf voltage	V
T_d	Disturbance torque externally applied to inertial load	N m
T_m	Torque generated by motor	N m
i_m	Motor armature current	A
i_f	Motor field current	A
k_m	Motor torque constant	N m A^{-1}
R_m	Motor armature resistance	Ω
L_m	Motor armature inductance	mH
J_m	Moment of inertia of motor rotor	kg m^2
J_l	Moment of inertia of inertial load	kg m^2
J_{eq}	Total moment of inertia of motor rotor and load	kg m^2
K	Open-loop steady-state gain	$\text{rad V}^{-1} \text{s}^{-1}$
τ	Open-loop time constant	s
M_l	Inertial load disc mass	kg
R_l	Inertial load disc radius	m
s	Laplace operator	rad s^{-1}
t	Continuous time	s

3 Prelab questions

Individual prelabs are attached at the end of this report.

4 Results and discussion

Sections 4.1, 4.2, and 4.3 use static conditions to determine physical properties of the DC motor and parameters of its associated transfer function. Section 4.5 uses measured system input and output under dynamic conditions to determine the transfer function parameters. The parameters derived from the prelab, static conditions and dynamic conditions are compared in Section 4.6.

4.1 Initial experimental tests

The motor described in the lab manual [1] is meant to be roughly equivalent to the motor used in the experiment. One notable difference is that the lab manual motor has a maximum u_m of 15 V DC. The QICii software used to control the experiment motor only allows a maximum u_m of 5 V DC. To establish the validity of the lab manual motor parameters as approximations for the experiment motor we will compare the $\omega_{m \max}$ from each source.

Using KVL in Figure 1, we can derive the relationship between the input voltage and the motor angular velocity as

$$u_m(t) = R_m i_m(t) + L_m \frac{\partial i_m(t)}{\partial t} + k_m \omega_m. \quad (2)$$

Since $i_m(t) \approx 0$ A at steady state, (2) can be simplified and evaluated with the parameters from the manual

$$\omega_{m \max} = \frac{u_{m \max}}{k_m} = \frac{15 \text{ V}}{0.0502 \text{ V s rad}^{-1}} = 298.8 \text{ rad s}^{-1}.$$

For the experiment motor, $\omega_{m \max}$ can be obtained directly from the QICii software. The response for $u_{m \max} = 5$ V is shown in Figure 2.

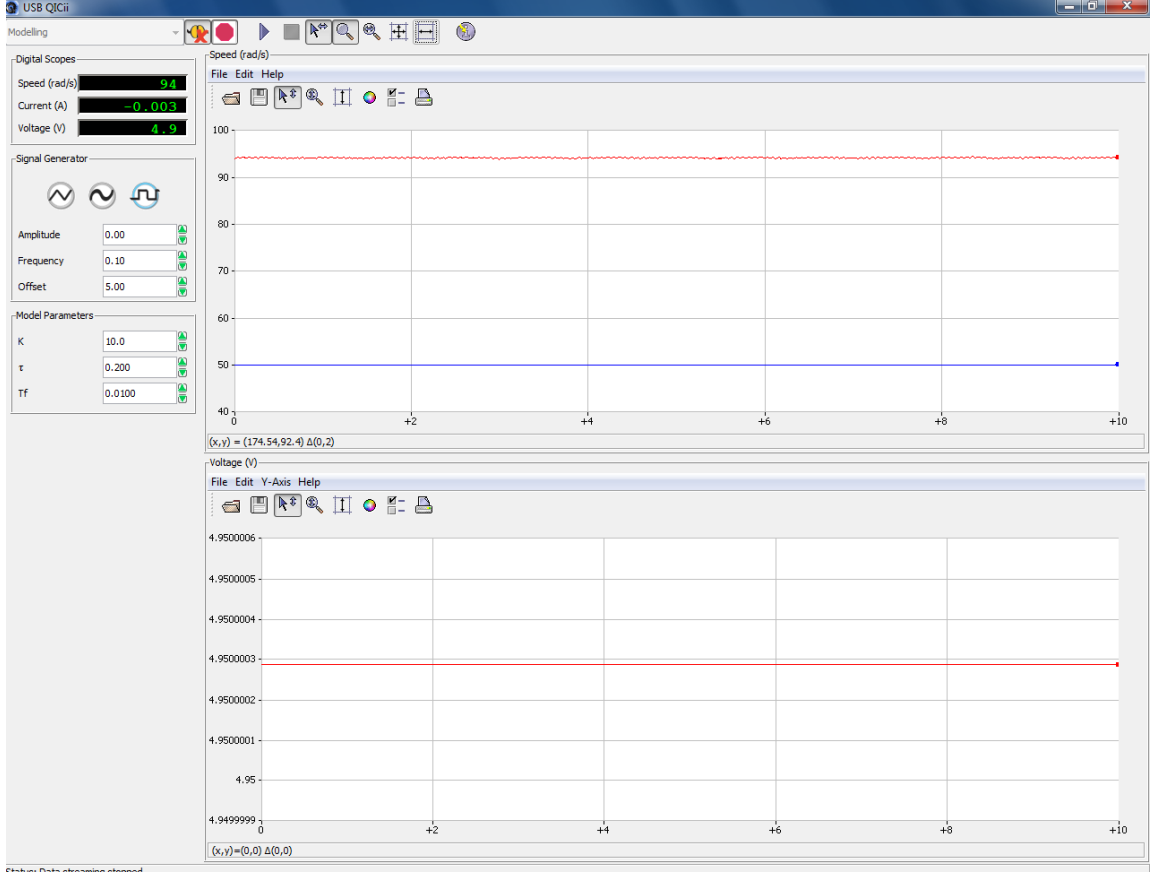


Figure 2: Steady state response of DC motor to constant u_m

For the experiment motor

$$k_m = \frac{4.95 \text{ V}}{94 \text{ rad s}^{-1}} = 0.05266 \text{ V s rad}^{-1}$$

which is slightly larger than the k_m in the lab manual. Thus, the physical parameters in the lab manual are valid. The difference between the two sets of parameters will be explored in Section 4.6.

4.2 Motor resistance

If $\omega_m = 0$ in (2) then we can determine R_m by measuring i_m . This constraint is realized by holding the disc stationary while applying different u_m . Note, a bias current, $i_{m \text{ bias}} = -10 \text{ mA}$ was measured when $u_m = 0 \text{ V}$. The R_m in each case is derived from (2) as

$$R_m = \frac{u_m}{i_m - i_{m \text{ bias}}}$$

Table 2 summarizes these results.

Table 2: Motor voltage and current at steady state

u_m (V)	i_m (A)	R_m (Ω)
−5.00	−0.35	14.3
−2.00	−0.15	13.3
1.00	0.05	20.0
2.00	0.13	15.4
5.00	0.33	15.2
$R_{m\,avg}$		15.6

The $R_{m\,avg}$ is nearly 50% larger than the value of $10.6\,\Omega$ used for calculations in the prelab. The source of this error can be seen in Figure 1. R_m is modeled as a lumped component but it represents the distributed resistance in the wires *and* the motor. The motor will experience a non-linear Coulomb friction at low voltages which this model lumps in to R_m . The non-linear nature of the R_m manifests as a spike at 1 V. Thus, the assumption that R_m is constant and the motor is frictionless cause an underestimation in the prelab values.

4.3 Motor torque constant

Similar to the approach in Section 4.2, we can determine k_m by analyzing the opposite static condition of the motor. When the motor is in a steady state of motion, $i_m \approx 0$. Using (2), we can determine

$$k_m = \frac{u_m}{\omega_m}.$$

Table 3 summarizes the results, with u_m varied over the same range as Section 4.2.

Table 3: Motor angular velocity in a free-spinning motor

u_m (V)	ω_m (rad s ^{−1})	k_m (V s rad ^{−1})
−5.00	−93	0.0538
−2.00	−35	0.0571
1.00	16	0.0625
2.00	35	0.0571
5.00	92	0.0543
$k_{m\,avg}$		0.0570

This is larger than the prelab value of $k_m = 0.0502\,\text{V s rad}^{-1}$. This is because the prelab model underestimates R_m and, since the motor does not perfectly conserve energy, ω_m will be slower than expected because of energy loss to friction and internal resistance.

4.4 Open loop transfer function parameters from static analysis

Taking the Laplace transform of (2) we can derive a first order transfer function of the form in (1), where the open loop transfer function $G(s) = \frac{\Omega_m(s)}{U_m(s)}$.

$$U_m(s) = R_m I_m(s) + s L_m I_m(s) + k_m \Omega_m(s) \quad (3)$$

[1] tells us that

$$J_{eq} \dot{\omega}_m(t) = k_m i_m(t) + T_d.$$

Disturbance torques can be neglected by ensuring the motor spins without interruption in the laboratory. The previous equation can be written in the Laplace domain as

$$s J_{eq} \Omega_m(s) = k_m I_m(s). \quad (4)$$

Substituting (4) into (3) yields

$$\frac{\Omega_m(s)}{U_m(s)} = \frac{k_m}{L_m J_{eq} s^2 + R_m J_{eq} s + k_m^2}.$$

For a small motor $R_m \gg L_m$, so the effect of L_m can be neglected in our linear model. The previous equation can be rewritten as

$$\frac{\Omega_m(s)}{U_m(s)} = \frac{1}{k_m \left(\frac{J_{eq} R_m}{k_m^2} s + 1 \right)}.$$

Comparing the previous equation with the form of (1) implies

$$K = \frac{1}{k_m} \quad \text{and} \quad \tau = \frac{J_{eq} R_m}{k_m^2}. \quad (5)$$

[1] gives values for J_m , M_l and R_l which can be used to determine J_{eq} .

$$\begin{aligned} J_{eq} &= J_m + \frac{1}{2} M_l R_l^2 \\ &= (11.6 \text{ g cm}^2) + \frac{1}{2} (68 \text{ g}) (2.48 \text{ cm})^2 \\ &= 220.7 \text{ g cm}^2 \\ &= 2.207 \times 10^{-5} \text{ kg m}^2 \end{aligned}$$

J_{eq} , $k_{m\,avg}$ and $R_{m\,avg}$ can be substituted into (5) to yield $K = 17.55 \text{ rad V}^{-1} \text{ s}^{-1}$ and $\tau = 0.106 \text{ s}$. The prelab has $K = 19.92 \text{ rad V}^{-1} \text{ s}^{-1}$ and $\tau = 0.093 \text{ s}$. The smaller gain and larger time constant represent the losses in the system to internal resistance and friction as well as the effect of L_m to inhibit motor acceleration.

4.5 Bump test

K and τ can also be derived by only measuring the input u_m and output ω_m during the application of a step input. This technique is referred to as a “bump test.” Assuming the measured system has a first order response, the output will be

$$y(t) = \Delta u K \left(1 - e^{-\frac{t}{\tau}} \right). \quad (6)$$

K will be the ratio of steady state output to input

$$K = \frac{\Delta y}{\Delta u}. \quad (7)$$

Substituting (7) into (6) at $t = \tau$ gives

$$y(\tau) = \Delta y (1 - e^{-1}) \approx 0.63 \Delta y. \quad (8)$$

The step input u_m will be approximated by a square wave varying between 1 V and 5 V ($\Delta u = 4 \text{ V}$) and a frequency of 0.4 Hz. The period between edges is long enough so that the motor will achieve its steady state behavior. Figure 3 shows the response of the DC motor to this input.

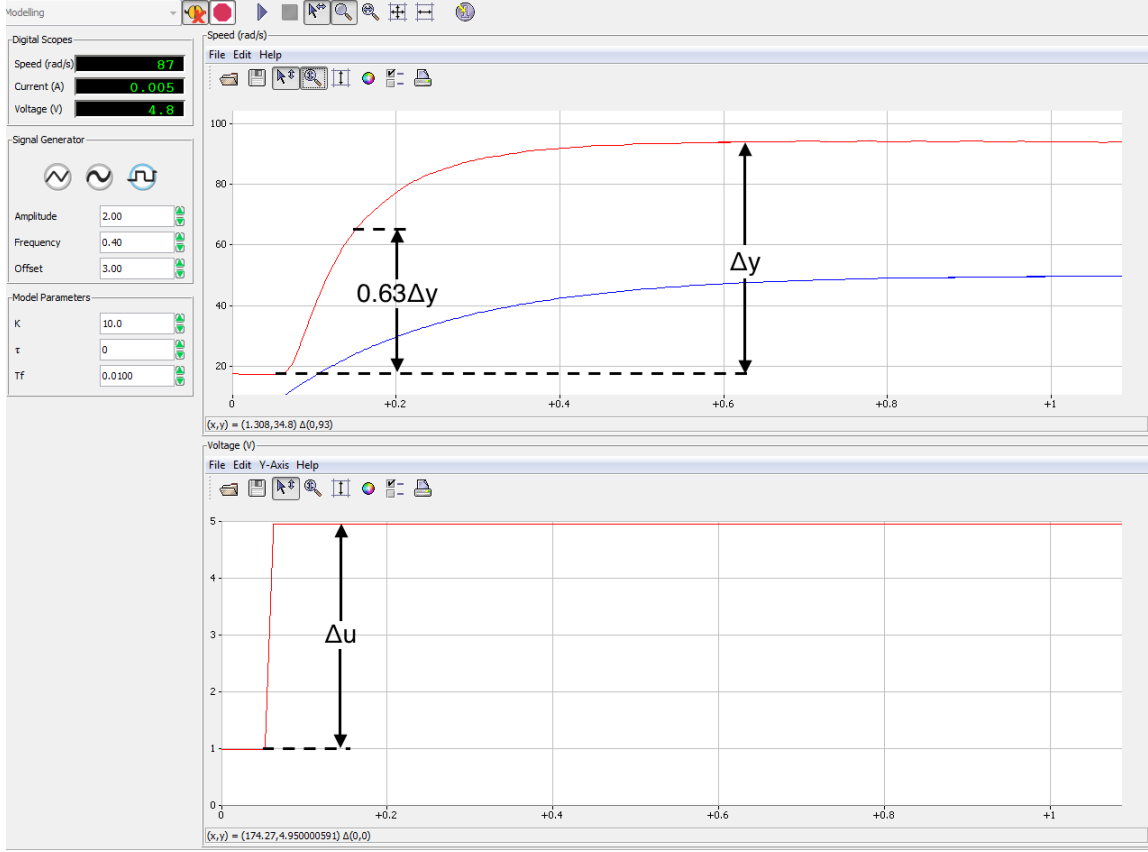


Figure 3: Response of DC motor to step input

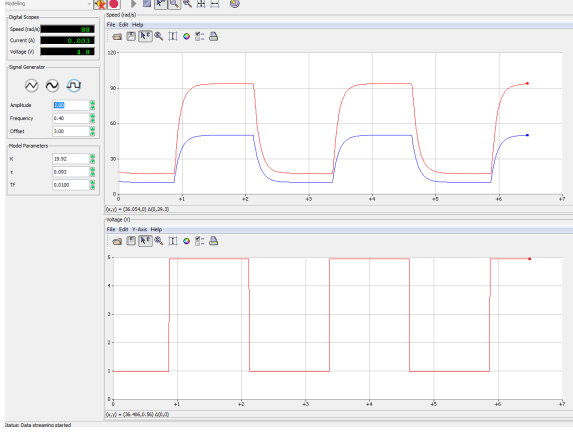
The response of the motor is $\Delta y = 75 \text{ rad s}^{-1}$. It reaches $0.63\Delta y$ at $\Delta t = 0.091 \text{ s} = \tau$. (7) gives $K = 18.75 \text{ rad V}^{-1} \text{ s}^{-1}$. These values are closer to the prelab values than those in Section 4.4.

4.6 Model validation

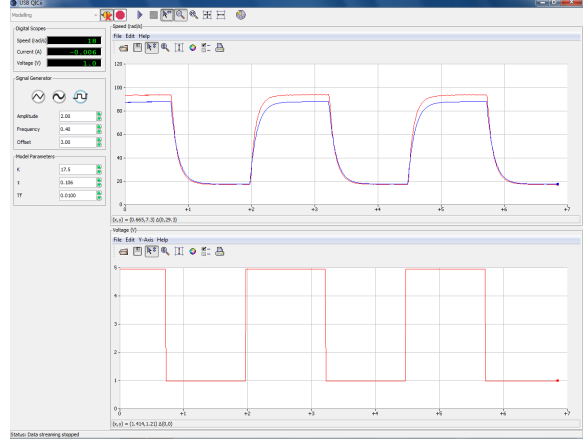
QUCii will take values of K and τ and use them to generate an expected response to the measured input. The square wave from Section 4.5 is reused as a step input. Figure 4 shows models with parameters derived from the prelab, static analysis and bump test. The model parameters in Figure 4(d) were determined by the best fit from manual parameter variation. The expected response is in dark blue and the measured response is in red.

The performance of the models is inversely correlated to the number of assumptions they make about the physical system at hand. The prelab values of R_m and k_m did not precisely match those from Sections 4.2 and 4.3 and its model is the furthest from the actual behavior of the motor.

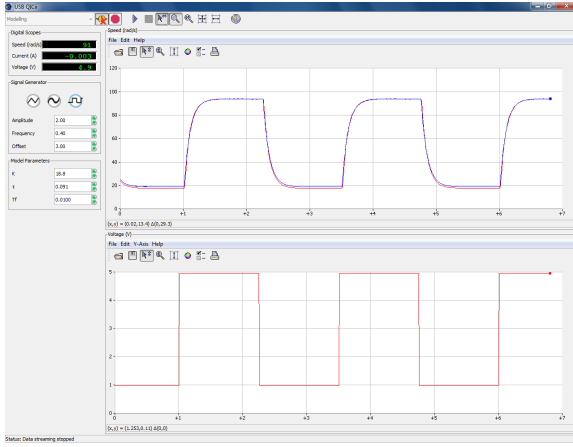
The model derived from static analysis ignored the effects of L_m and T_d entirely and i_m and



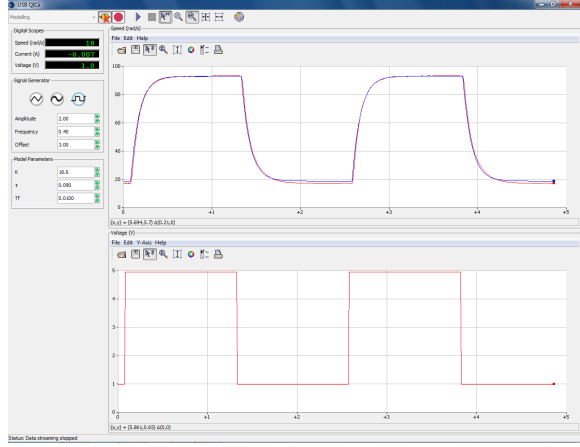
(a) Prelab: $K = 19.92 \text{ rad V}^{-1} \text{ s}^{-1}$, $\tau = 0.93 \text{ s}$



(b) Static analysis: $K = 17.5 \text{ rad V}^{-1} \text{ s}^{-1}$, $\tau = 0.106 \text{ s}$



(c) Bump test: $K = 18.8 \text{ rad V}^{-1} \text{ s}^{-1}$, $\tau = 0.091 \text{ s}$



(d) Tuned: $K = 18.6 \text{ rad V}^{-1} \text{ s}^{-1}$, $\tau = 0.090 \text{ s}$

Figure 4: Performance of various models against measured motor response to step input

ω_m when it was convenient. The static analysis model performs considerably better than the prelab model but it underestimates the motor response at the upper steady state.

The bump test model performs extremely well. It tracks the “up” response perfectly. The model deviates very slightly on the “down” response, where it fails to track the observed decay of ω_m at steady state. This deviance is likely due to a breakdown of the linear model as $u_m \rightarrow 0.4 \text{ V}$, the voltage at which the motor overcomes the Coulomb friction and begins to rotate. Observe the spike in R_m in Table 2 at $u_m = 1.00 \text{ V}$. This suggests Coulomb friction is significant over a range of values and manifests as non-linear behavior at low voltages.

The tuned model is not a significant improvement over the bump test model. This is because the non-linearities from Coulomb friction cannot be accounted for by varying K and τ in a linear model.

5 Conclusion

In this experiment we were able to derive three different sets of parameters for the model of the DC motor. The parameters derived from the prelab calculations did a poor job of approximating the motor's behavior because they make incorrect assumptions about the value of R_m and k_m of the motor. Measurements of the motor in static conditions and parameter derivation from physical relations provided parameters for an adequate model. However, the assumptions that L_m and T_d were non-existent result in a consistent underestimation of the motor's maximum angular velocity. The parameters derived from the bump test, $K = 18.8 \text{ rad V}^{-1} \text{ s}^{-1}$ and $\tau = 0.091 \text{ s}$, almost perfectly model the behavior of the motor. The model does not account for the decline in velocity at low voltages because it ignores the Coloumb friction in the motor which is greatest around $\pm 0.4 \text{ V}$ and negligible beyond 2 V . Manual tuning of K and τ could not significantly improve on the accuracy of the bump test parameters.

This experiment did not investigate the model's behavior at the upper end of its validity: where a large enough u_m is supplied so that the gain becomes saturated. Future experiments with this motor must take into account the existence of this upper limit. The model parameters we have derived will be most accurate when u_m has an operational range of 2 V to 5 V .

References

- [1] P. Agathoklis, *Laboratory Manual for ELEC 360 - Control Systems I*, University of Victoria, 2016.